

Received 19 October 2023, accepted 8 November 2023, date of publication 14 November 2023,
date of current version 27 November 2023.

Digital Object Identifier 10.1109/ACCESS.2023.3332992

RESEARCH ARTICLE

58-nW 0.5-V Mixed-Mode Universal Filter Using Multiple-Input Multiple-Output OTAs

FABIAN KHATEB^{1,2,3}, MONTREE KUMNGERN⁴, AND TOMASZ KULEJ⁵

¹Department of Microelectronics, Brno University of Technology, 601 90 Brno, Czech Republic

²Faculty of Biomedical Engineering, Czech Technical University in Prague, 272 01 Kladno, Czech Republic

³Department of Electrical Engineering, University of Defence, 662 10 Brno, Czech Republic

⁴Department of Telecommunications Engineering, School of Engineering, King Mongkut's Institute of Technology Ladkrabang, Bangkok 10520, Thailand

⁵Department of Electrical Engineering, Częstochowa University of Technology, 42-201 Częstochowa, Poland

Corresponding author: Montree Kumngern (montree.ku@kmitl.ac.th)

This work was supported by the University of Defence, Brno, within the Organization Development Project Military Autonomous and Robotic Assets (VAROPS).

ABSTRACT This paper presents a mixed-mode universal filter using a multiple-input multiple-output operational transconductance amplifier (MIMO-OTA). The multiple-input OTA is designed using the multiple-input MOS transistor technique (MI-MOST), resulting in a single differential pair and minimal power consumption. The MIMO-OTA is used to design a universal mixed-mode filter that provides input and output in voltage and current form. In a single topology, second order filters with low-pass (LP), high-pass (HP), band-pass (BP), band-stop (BS) and all-pass (AP) transfer functions can be obtained in voltage-mode (VM), current-mode (CM), transadmittance-mode (TAM) and transimpedance-mode (TIM). In addition, VM, CM, and TAM offer non-inverting and inverting transfer functions of LP, HP, BP, BS, and AP filters. The natural frequency and quality factor of all filter functions can be orthogonally controlled. Electronic tuning of the natural frequency is provided. The supply voltage is 0.5 V and the power consumption of the filter is 58 nW for 4 nA setting current. The filter was designed and simulated in the Cadence Virtuoso environment using TSMC 0.18 μ m CMOS technology. The simulation results including Monte-Carlo analysis and process, voltage, and temperature corners are presented.

INDEX TERMS Universal filter, analog filter, operational transconductance amplifiers, multiple-input MOS transistor.

I. INTRODUCTION

Mixed-mode analog circuits are electronic circuits that process signals in both current and voltage modes. The input of the circuit can be supplied by a current or voltage signal and the output of the circuit offers a voltage or current signal. Such circuits are needed for example when voltage-mode (VM) circuits are combined with current-mode (CM) circuits. These circuits may operate in transadmittance-mode (TAM) when a voltage signal is supplied to the input and the output is a current signal. They may also operate in transimpedance-mode (TIM) when a current signal is supplied to the input and the output is a voltage signal.

In the field of universal filters, mixed-mode universal filters are circuits that can provide four modes - VM, CM, TAM

The associate editor coordinating the review of this manuscript and approving it for publication was Dušan Grujić.

and TIM - in one circuit, with each mode offering five filter responses: low-pass (LP), high-pass (HP), band-pass (BP), band-stop (BS), and all-pass (AP). Thus, a perfect universal mixed-mode filter could have a total of twenty transfer functions in a single circuit. Mixed-mode universal filters such as TAM and TIM can be easily connected to realize higher order filters and they can offer many filter transfer functions if they are fabricated as integrated circuits (ICs). Many mixed-mode universal filters based on different active devices are available in open literature [1], [2], [3], [4], [5], [6], [7], [8], [9], [10], [11], [12], [13], [14], [15], [16], [17], [18], [19], [20], [21], [22], [23], [24], [25], [26], [27], [28], [29], [30], [31], [32], [33], [34], [35], [36], [37], [38]. The circuits in [1], [2], [3], [4], [5], [6], [7], [8], [9], and [10] use current conveyors, the circuits in [11], [12], and [13] use a current feedback amplifier (CFA), and the circuit in [14] uses a four-terminal

floating nullor (FTFN). However, these filters lack electronic tuning capability.

Circuits with electronic tuning capabilities have been designed using current-controlled current conveyors [15], [16], [17], [18], voltage-differencing transconductance amplifiers (VDTA) [19], current-conveyor transconductance amplifiers (CCTA) [20], [21], [22], [23], or voltage differencing differential voltage current conveyors (VD-DVCC) [24], [25]. With respect to the input and output terminals, several circuits, such as those in [15], [17], [18], [24], and [25], are classified as multiple-input multiple-output (MIMO) filters that use fewer active devices. However, these filters suffer from certain disadvantages, e.g., they do not provide twenty transfer functions in the same circuit [15], [16], [18], [19], [20], [21], [23], they use input signal or passive components matching conditions [17], [18], [21], [24], [25], or they apply the input signal through a capacitor or resistor, requiring an additional buffer circuit [18], [19], [21], [24].

In the last decade, many universal filters using an operational transconductance amplifier (OTA) as the active element have been proposed. This device offers some advantages in circuit design, such as the possibility of electronic tuning and design simplicity. OTA-based circuits do not require any resistors, making them suitable for monolithic integration. Many OTA-based universal mixed-mode filters have been introduced [26], [27], [28], [29], [30], [31], [32], [33], [34], [35]. However, the filters in [26], [27], [28], [29], [30], and [31] do not provide the full capability of a universal mixed-mode filter, namely twenty transfer functions in the same circuit. The circuits in [32], [33], [34], and [35] offer twenty transfer functions, but these OTA structures are not designed for low-voltage and low-power applications. New active devices, such as the voltage differencing buffered amplifier (VDBA), the voltage differencing gain amplifier (VDGA) and the differential difference transconductance amplifier (DDTA) [36], [37], [38], and [39], have been used to implement universal mixed-mode filters, but the filters in [36], [37], [38], and [39] use supply voltages of ± 1.25 V, ± 0.75 V, ± 0.9 V, and 1.2 V, respectively. Nowadays, low-power consumption is important for circuit designers because low power consumption circuits are required for applications in portable electronics, sensors and biomedical systems.

Multiple-input active analog building blocks, such the differential difference amplifier (DDA) [40], [41], [42], [43], [44], the differential difference current conveyor (DDCC) [45], [46], the differential difference operational floating amplifier (DDOFA) [47] and the multiple-input operational transconductance amplifier (MI-OTA) [48], [49], [50], [51], have been found to be attractive solutions for reducing the number of applications blocks and thus power consumption. They are used for signal processing and analog computation and are designed to handle differential and difference signals. Therefore, they are widely used in instrumentation, analog computing circuits, active filters, sensor interfaces, and communication systems. However, the internal transistor structures of the multiple-input blocks are more complex

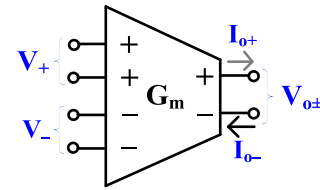


FIGURE 1. Electrical symbol of the MIMO-OTA.

due to the increased number of differential pairs and current branches, which leads to an increase in power consumption and chip area compared to the standard design using a single differential pair. To maintain a single differential pair with multiple-inputs, a MOS transistor with multiple inputs (MI-MOST) is the solution [52], [53], [54], [55], [56], [57], [58], [59], [60], [61], [62], [63], [64], [65], [66]. The first experimental results of MI-MOST implementation were presented in [52], [53], [54], and [55] and its various applications were presented in [56], [57], [58], [59], [60], [61], [62], [63], [64], and [65].

This paper presents a new application of a mixed-mode universal filter using multiple-input multiple-output operational transconductance amplifiers. The MIMO-OTA gives extended capability of a mixed mode filter by offering the five standard filtering functions in four modes: VM, CM, TIM, and TAM. The filter is suitable for low frequency applications that require extremely low-voltage supply and low-power consumption, such as portable biomedical and energy harvesting sensor devices.

This paper is organized as follows: Section II describes the multiple-input/output OTA, the applications of the mixed-mode universal filter and non-ideality analysis. Section III presents the simulation results. Finally, the conclusion is given in Section IV.

II. PROPOSED CIRCUIT

A. THE MULTIPLE-INPUT MULTIPLE-OUTPUT OTA

The circuit symbol and the CMOS realization of the MIMO-OTA, used to realize the universal filter proposed in this work, are shown in Figs. 1 and 2, respectively. Its characteristic behavior, in an ideal case, is described by:

$$I_{o\pm} = \pm g_m \left(\sum_{i=1}^n V_{+i} - \sum_{i=1}^n V_{-i} \right) \quad (1)$$

where n is the number of inputs of the MIMO-OTA. For the purposes of this work, $n = 2$.

The multiple-input OTA, with one positive current output, was first presented and experimentally verified in [55]. The structure was then used in several applications [56], [57], [58]. In this work, for the aim of the presented application, the circuit was equipped with an extra negative current output. Thus, the OTA possessed a differential current output that extended its universality.

Overall, the circuit can be seen as a current mirror OTA, with the input bulk-driven (BD) pair M_1 - M_2 . In order to increase its linear range, the BD transistors M_{11} - M_{12} ,

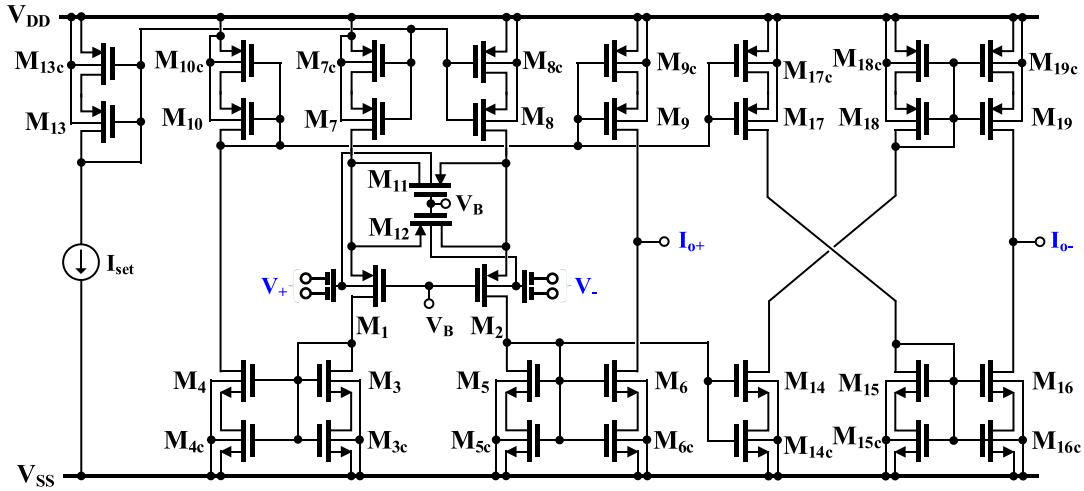


FIGURE 2. CMOS structure of the MIMO-OTA.

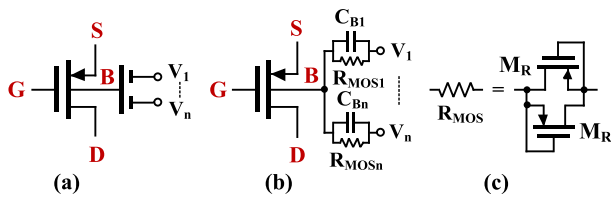


FIGURE 3. MI-BD MOST technique: (a) symbol, (b) realization, (c) implementation of R_{MOS} .

operating in the triode region, were added. The input stage can therefore be seen as a BD counterpart of the Krummenaher and Joehl transconductor [67] but operating in weak inversion. Note that with the use of BD transistors, both the input differential range and the input common-mode range are extended in comparison to the gate-driven counterpart of the presented structure [55].

The large-signal differential output current of the input stage, operating in weak inversion, can be expressed as [55]:

$$I_{D1} - I_{D2} = 2I_{set} \tanh \left(\eta \frac{V_{bd}}{2n_p U_T} - \tanh^{-1} \left[\frac{1}{4m+1} \tanh \left(\eta \frac{V_{bd}}{2n_p U_T} \right) \right] \right) \quad (2)$$

where $h = (n_p - 1) = g_{mb1,2}/g_{m1,2}$ at the operating point, n_p is the subthreshold slope factor for the p-channel transistors, U_T is the thermal potential, I_{set} is the quiescent drain current of M_1 and M_2 , g_m and g_{mb} is the gate and the bulk transconductance respectively, $m = (W_{11,12}/L_{11,12})/(W_{1,2}/L_{1,2})$ is the relative aspect ratio of the two matched transistor pairs $M_{11,12}$ and $M_{1,2}$, and V_{bd} is the differential voltage between the bulk terminals of the input transistors M_1 and M_2 .

The linearity of the input stage depends on the coefficient m , which for optimum linearity should be equal to 0.5 [55]. This result does not depend on the biasing current I_{set} .

The bulk terminals of the input transistors are connected to the inputs of the OTA via the capacitive voltage divider shown in Fig. 3. Note that the BD MOS transistor equipped

with such a divider can be seen as a new active device called a multiple-input BD MOS transistor [52]. The large resistors R_{MOS} , formed through the anti-parallel connection of two minimum-size MOS transistors operating in the cutoff region with $V_{GS} = 0$, are used to provide proper biasing of the bulk terminal for DC. For larger frequencies, the voltages at the bulk terminals of the input transistors M_1 and M_2 can be expressed as:

$$V_{b1,2} = \sum_{i=1}^n \beta_i V_{+,-i} \quad (3)$$

where b_i is the voltage gain of the input capacitive divider, for a general case given as:

$$\beta_i = \frac{C_{Bi}}{\sum_{i=1}^n C_{Bi}} \quad (4)$$

Note that in this paper, $b_1 = b_2 = b$.

Utilizing MI-BD MOS transistors simplifies the MI-OTA structure, i.e., it realizes the needed arithmetic function without applying an additional differential pair. This leads to power reduction as well.

The output currents of the input pair are conveyed to the non-inverting (I_{o+}) and inverting (I_{o-}) outputs via the current mirrors based on transistors M_3 - M_{19} . In order to increase their output resistances, and consequently the DC voltage gain of the MIMO-OTA, while not limiting the output voltage range in an ultra-low-voltage environment, the mirrors are based on self-cascode transistors.

Using (2) and (4) and assuming unity-gain current mirrors, the small-signal transconductance of the MIMO-OTA can be expressed as:

$$\beta g_m = \cdot \eta \cdot \frac{4m}{4m+1} \cdot \frac{I_{set}}{n_p U_T} \quad (5)$$

while its DC differential voltage gain can be approximated as:

$$A_{VO} \cong 2g_m [(g_{m9} r_{ds9} r_{ds9c}) || (g_{m6} r_{ds6} r_{ds6c})] \quad (6)$$

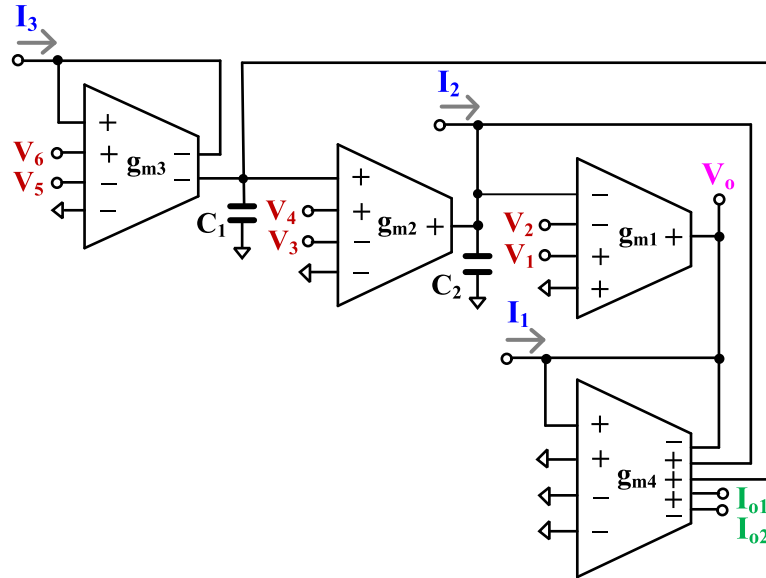


FIGURE 4. Proposed mixed-mode universal filter using MIMO-OTAs.

Assuming identity of all current mirrors of the same type, the output noise currents of the MIMO-OTA can be expressed as:

$$\overline{I_{no+}^2} = 2\overline{I_{n1,2}^2} \left(\frac{2G}{g_{m1,2} + 2G} \right)^2 + 2\overline{I_{np}^2} \left(\frac{g_{m1,2}}{g_{m1,2} + 2G} \right)^2 + \overline{I_{nG}^2} \left(2 \frac{g_{m1,2}}{g_{m1,2} + 2G} \right)^2 + 4\overline{I_{nn}^2} + 2\overline{I_{np}^2} \quad (7)$$

$$\overline{I_{no-}^2} = 2\overline{I_{n1,2}^2} \left(\frac{2G}{g_{m1,2} + 2G} \right)^2 + 2\overline{I_{np}^2} \left(\frac{g_{m1,2}}{g_{m1,2} + 2G} \right)^2 + \overline{I_{nG}^2} \left(2 \frac{g_{m1,2}}{g_{m1,2} + 2G} \right)^2 + 6\overline{I_{nn}^2} + 4\overline{I_{np}^2} \quad (8)$$

where $\overline{I_{nG}^2}$ is the noise current of the triode operating transistors M_{11}, M_{12} :

$$\overline{I_{nG}^2} = 4kTG + 2 \frac{Kg_m^2}{fC_{OX}WL_{11,12}} \quad (9)$$

where G is the drain-source conductance of M_{11} and M_{12} at the operating point, and $\overline{I_{nn}^2}$ and $\overline{I_{np}^2}$ are the noise currents of the self-cascode transistors of the n- and p-type current mirrors respectively. These are approximately equal to the noise of their upper transistors in weak inversion:

$$\overline{I_{nn,p}^2} = 2qI_D + \frac{1}{fC_{OX}} \left(\frac{Kg_m^2}{WL} \right) \quad (10)$$

where I_D is the drain current (in this design it is equal to I_{set}), q is the electron charge, C_{OX} is the oxide capacitance per unit area and K is the flicker noise constant (different for n- and p-channel transistors). Note that the same equation describes the noise currents of the transistors M_1 and M_2 ($\overline{I_{n1,2}^2}$).

The input referred noise, with respect to the corresponding output, can be calculated as:

$$\overline{\beta v_{n+,-}^2} = \frac{\overline{I_{no+,-}^2}}{g_m^2} = \frac{\overline{I_{no+,-}^2}}{\left(\eta \cdot \frac{4m}{4m+1} \cdot \frac{I_{set}}{n_p U_T} \right)^2} \quad (11)$$

As can be concluded from (4)-(11), the input capacitive divider decreases both the input transconductance and the DC voltage gain of the OTA. The input capacitive divider also extends the linear range and input noise by the same amount; therefore, the dynamic range remains the same for the OTA with and without the input capacitive divider [55].

To sum up, the proposed technique simplifies the structure and reduces its dissipation power while maintaining its dynamic range. The above advantages are achieved at the cost of a lower voltage gain. However, thanks to the application of other low-voltage techniques, like the self-cascode technique, the achieved voltage gain is sufficient for the proposed application.

B. MIXED-MODE UNIVERSAL FILTER USING MIMO-OTA

Fig. 4 shows the proposed mixed-mode universal filter using MIMO-OTA. The circuit uses four MIMO-OTAs and two grounded capacitors. All input voltage terminals and all output current terminals have a high impedance level; hence, no additional buffering circuitry is needed. The output impedance of the voltage terminal V_o can be given by $1/g_{m4}$. Using (1) and nodal analysis, the outputs V_o, I_{o1} and I_{o2} can be specified as:

$$V_o = \frac{g_{m1}}{g_{m4}} \cdot \frac{s^2 C_1 C_2 (V_1 - V_2) + s C_1 g_{m2} (V_3 - V_4) + g_{m2} g_{m3} (V_5 - V_6)}{s^2 C_1 C_2 + s C_1 g_{m1} + g_{m1} g_{m2}} \quad (12)$$

TABLE 1. Obtaining variant filtering functions of the proposed mixed-mode universal filter.

Mode Operation	Filtering Function		Input	Output	
VM	HP	Non-inverting	V_1	V_o	
		Inverting	V_2	V_o	
	BP	Non-inverting	V_3	V_o	
		Inverting	V_4	V_o	
	LP	Non-inverting	V_5	V_o	
		Inverting	V_6	V_o	
	BS	Non-inverting	$V_1 = V_5$	V_o	
		Inverting	$V_2 = V_6$	V_o	
	AP	Non-inverting	$V_1 = V_4 = V_5$	V_o	
		Inverting	$V_2 = V_3 = V_6$	V_o	
CM	HP	Inverting	I_1	I_{o1}	
		Non-inverting	I_1	I_{o2}	
	BP	Non-inverting	I_2	I_{o1}	
		Inverting	I_2	I_{o2}	
	LP	Inverting	I_3	I_{o1}	
		Non-inverting	I_3	I_{o2}	
	BS	Inverting	$I_1 = I_3$	I_{o1}	
		Non-inverting	$I_1 = I_3$	I_{o2}	
	AP	Inverting	$I_1 = I_2 = I_3$	I_{o1}	
		Non-inverting	$I_1 = I_2 = I_3$	I_{o2}	
	TAM	HP	Non-inverting	V_1	I_{o1}
			Inverting	V_2	I_{o1}
BP		Non-inverting	V_3	I_{o1}	
		Inverting	V_4	I_{o1}	
LP		Non-inverting	V_5	I_{o1}	
		Inverting	V_6	I_{o1}	
BS		Non-inverting	$V_1 = V_5$	I_{o1}	
		Inverting	$V_2 = V_6$	I_{o1}	
AP		Non-inverting	$V_1 = V_4 = V_5$	I_{o1}	
		Inverting	$V_2 = V_3 = V_6$	I_{o1}	
TIM	HP	Inverting	I_1	V_o	
	BP	Non-inverting	I_2	V_o	
	LP	Inverting	I_3	V_o	
	BS	Inverting	$I_1 = I_3$	V_o	
	AP	Inverting	$I_1 = I_2 = I_3$	V_o	

TABLE 2. Transistor aspect ratio of the MIMO-OTA.

Component	W/L ($\mu\text{m}/\mu\text{m}$)
M_1, M_2	$2 \times 15/1$
$M_3-M_6, M_{14}-M_{16}$	$2 \times 10/1$
$M_{3c}-M_{6c}, M_{14c}-M_{16c}$	$10/1$
$M_7-M_{10}, M_{17}-M_{19}, M_{13}$	$2 \times 15/1$
$M_{7c}-M_{10c}, M_{17c}-M_{19c}, M_{13c}, M_{11}, M_{12}$	$15/1$
M_R	$5/4$
$C_B=0.5\text{pF}$	

$$I_{o1} = g_{m1} \cdot \frac{s^2 C_1 C_2 (V_1 - V_2) + s C_1 g_{m2} (V_3 - V_4) + g_{m2} g_{m3} (V_5 - V_6)}{s^2 C_1 C_2 + s C_1 g_{m1} + g_{m1} g_{m2}} \quad (13)$$

$$I_{o1} = -I_{o2} = \frac{-s^2 C_1 C_2 I_1 + s C_1 g_{m1} I_2 - g_{m1} g_{m2} I_3}{s^2 C_1 C_2 + s C_1 g_{m1} + g_{m1} g_{m2}} \quad (14)$$

$$V_o = \frac{1}{g_{m4}} \cdot \frac{-s^2 C_1 C_2 I_1 + s C_1 g_{m1} I_2 - g_{m1} g_{m2} I_3}{s^2 C_1 C_2 + s C_1 g_{m1} + g_{m1} g_{m2}} \quad (15)$$

The voltage gain of the VM filter can be given by g_{m1}/g_{m4} . The g_{m1} is used to convert the input voltages to the output current for the TAM filter, and the g_{m4} is used to convert the input current to the output voltage for the TIM. It is worth mentioning that when a single OTA can provide plus-and minus-type multiple-input and multiple-output terminals, the non-inverting and inverting transfer functions of LP, HP, BP, BS, and AP filters of VM, CM, and TAM can be easily obtained. Variant filtering functions of LP, HP, BP, BS, and AP filters of VM, CM, TAM, and TIM are obtained according

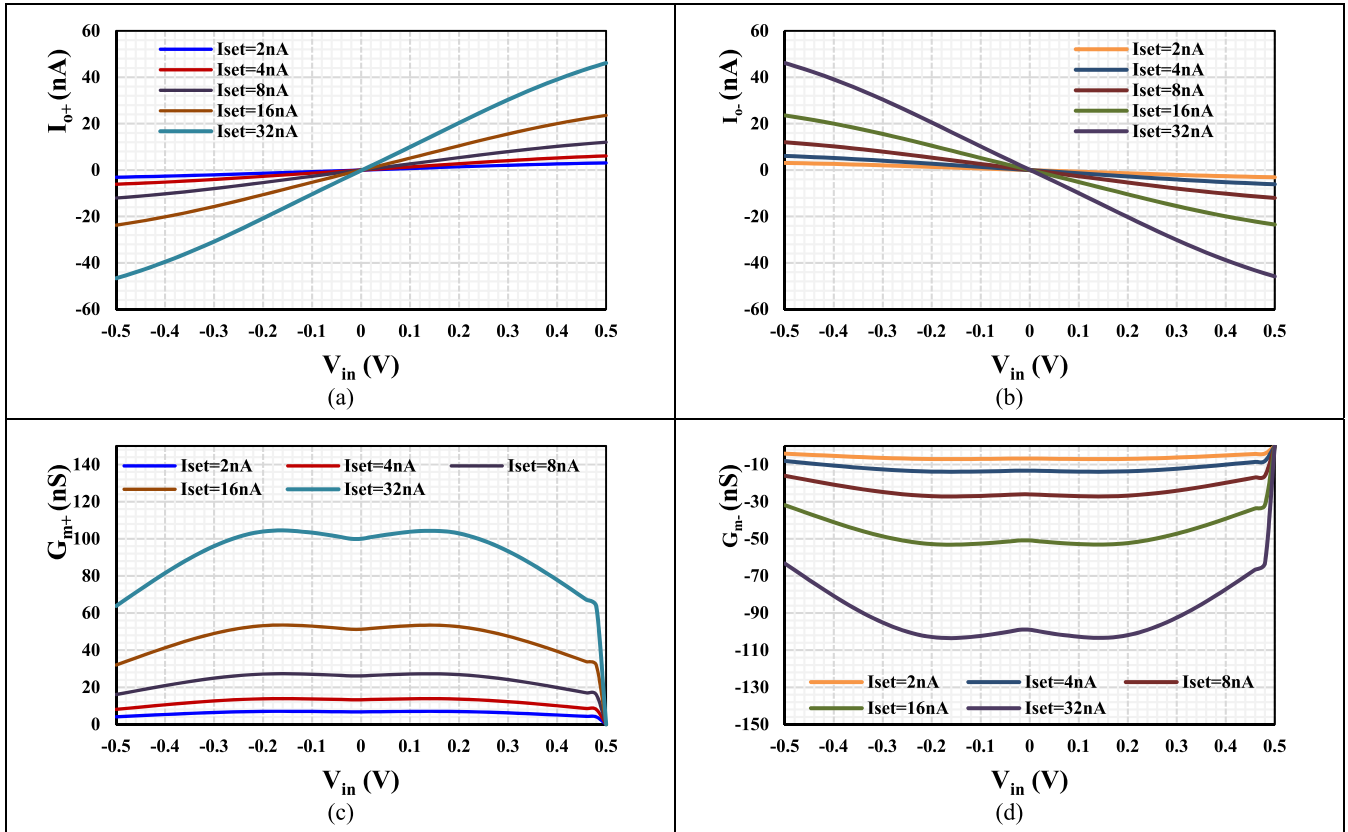


FIGURE 5. The DC characteristics of the MIMO-OTA: Output currents I_{o+} , I_{o-} (a,b) and small-signal transconductance G_{m+} , G_{m-} (c,d) for different I_{set} .

TABLE 3. Comparison of the proposed filter's properties with those of mixed-mode universal filters.

Features	Proposed	[5]	[17]	[18]	[23]	[35]	[37]	[39]
Number of active devices	4-OTA	3-DDCC	4-CCCII	1-EX-CCCII	3-CCCCTA	8-OTA	2-VDBA	5-DDTA
Realization	0.18 μ m CMOS	0.25 μ m CMOS	0.35 μ m CMOS	0.18 μ m CMOS	0.18 μ m CMOS	0.18 μ m CMOS	0.18 μ m CMOS	0.18 μ m CMOS
Number passive devices	2-C	2-C, 3-R	2-C	2-C, 1-C	2-C	2-C	2-C, 2-R	2-C
Type of filter	MIMO	MISO	MIMO	MISO	SIMO	MIMO	MIMO	MIMO
Total number of offered responses	35	30	20	17	22	20	17	36
Each mode offered five standard responses	Yes	Yes	Yes	No (TIM)	No (TIM)	Yes	No (TIM)	Yes
Orthogonal control of ω_o and Q	Yes	Yes	Yes	Yes	Yes	Yes	Yes	Yes
Electronic control of ω_o	Yes	No	Yes	Yes	Yes	Yes	Yes	Yes
All passive devices grounded	Yes	Yes	Yes	No	Yes	Yes	No	Yes
High input impedances for VM	Yes	Yes	Yes	No	Yes	Yes	No	Yes
Input matching conditions not needed	Yes	Yes	No	No	Yes	Yes	Yes	Yes
Inverting input conditions not needed	Yes	Yes	Yes	No	Yes	Yes	Yes	Yes
Power supply (V)	0.5	± 1.25	± 1.25	± 0.5	± 0.9	± 0.3	± 0.75	1.2
Power dissipation (mW)	58×10^{-3}	-	-	1.35	1.99	5.77×10^{-3}	0.373	0.33
Natural frequency (kHz)	114×10^3	3.315×10^3	-	23×10^3	3.183×10^3	5	1.44×10^3	1.04
Total harmonic distortion (%)	1@170mV _p	0.723@60 μ A _{pp}	0.5@150 μ A _{pp}	<0.2@100 mV _{pp}	2.16@500 mV _{pp}	2@120mV _{pp} (LP)	2.2@200mV _{pp}	1.09@650 mV _{pp}
Dynamic range (dB)	53.2	-	-	-	-	53.2	-	-
Verification of result	Sim	Sim	Sim	Sim/Exp	Sim	Sim	Sim/Exp	Sim/Exp

to Table 1. It can be seen that the filter offers 35 transfer functions without inverting input signal requirements. If the

circuit operates as VM and TAM, the input current terminals I_1 and I_2 can be floating and the input current I_2 must be

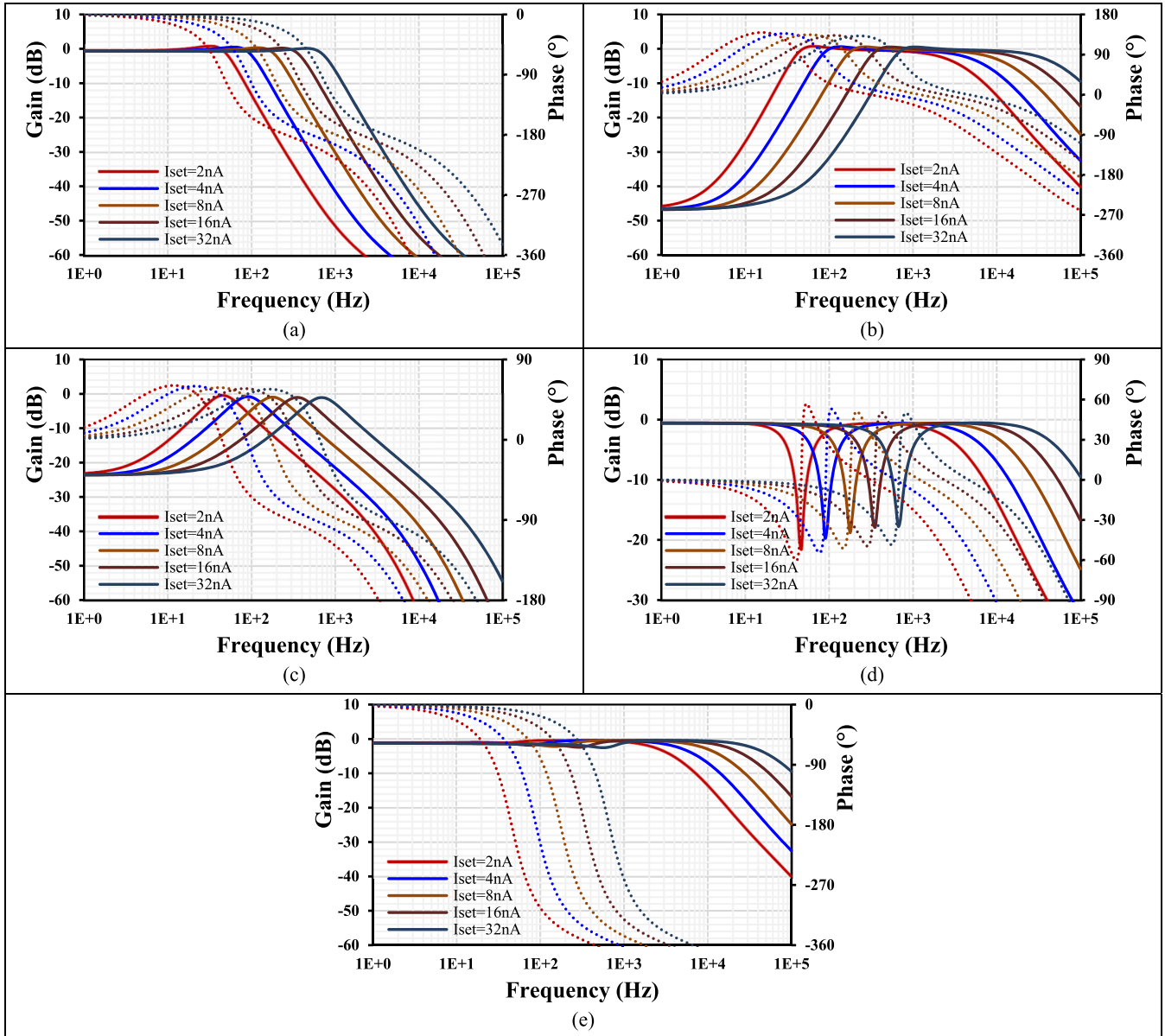


FIGURE 6. The frequency characteristics of gains (lines) and phases (points) for the VM filter: LPF (a), HPF (b), BPF (c), BSF (d), and APF (e).

connected to ground, while the input voltage terminals that are not used can be grounded.

The natural frequency (ω_o) and the quality factor (Q) can be given respectively as:

$$\omega_o = \sqrt{\frac{g_{m1}g_{m2}}{C_1C_2}} \quad (16)$$

$$Q = \sqrt{\frac{C_2g_{m2}}{C_1g_{m1}}} \quad (17)$$

Thus, the natural frequency can be electronically controlled by g_{m1} and g_{m2} (i.e., $g_{m1} = g_{m2}$) and the quality factor can be given by C_2/C_1 .

C. NON-IDEALITY ANALYSIS

A practical small signal OTA model in [68] is used to analyze the filter performance characterization. Three components should be characterized: (i) the differential-mode capacitance C_d and common-mode capacitance C_c , (ii) the output capacitance C_o and output conductance g_o , and (iii) the frequency-dependent transconductance that can be given [68] by:

$$g_m(s) \approx g_{mo}(1 - s\tau) \quad (18)$$

where g_{mo} is the transconductance of the ideal OTA, $\tau = 1/\omega_g$, and ω_g is the second pole of the OTA, which is given by the cut-off frequency of the OTA.

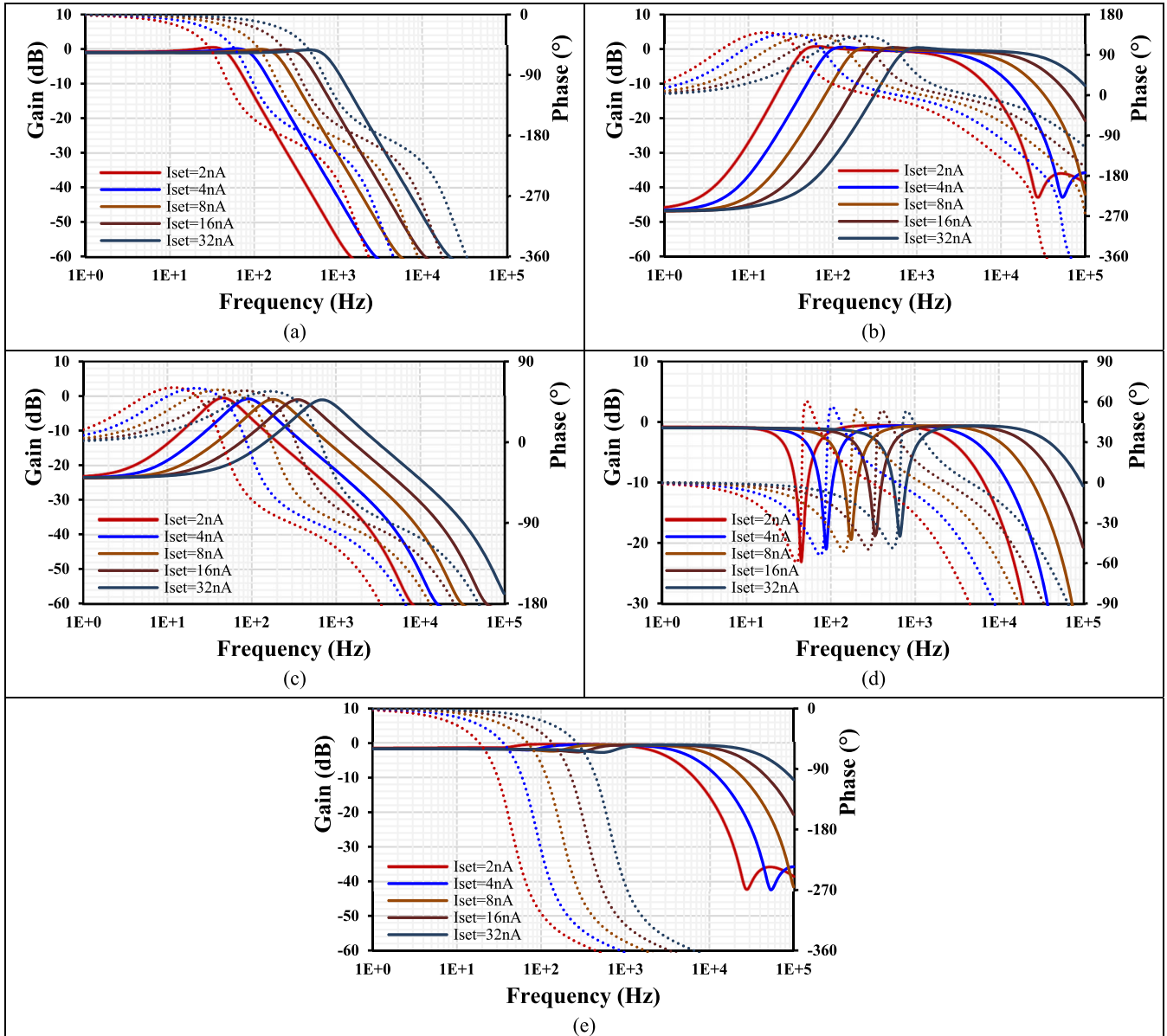


FIGURE 7. The frequency characteristics of gains (lines) and phases (points) for the CM filter: LPF (a), HPF (b), BPF (c), BSF (d), and APF (e).

From Fig. 4, the parasitic capacitances C_{03} , C_{04} , C_{c2} and parasitic conductances g_{03} and g_{04} are parallel with C_1 . The parasitic capacitances C_{02} , C_{04} , C_{c1} and parasitic conductances g_{02} and g_{04} are parallel with C_2 , where C_{02} , C_{03} , C_{04} are respectively the output capacitances of g_{m2} , g_{m3} , g_{m4} ; C_{c1} and C_{c2} are respectively the common-mode capacitances of g_{m1} and g_{m2} ; and g_{02} , g_{03} , g_{04} are respectively the output conductances of g_{m2} , g_{m3} , g_{m4} . The parasitic capacitances can be neglected by choosing appropriate values, such as C_1 , $C_2 \gg C_{0j}$, C_{cj} and $g_{mj} \gg g_{0j}$, where $j = 1, 2, 3, 4$ of g_{mj} .

The frequency-dependent transconductance in (17) was also considered; thus, the denominator of the proposed filter can be expressed by:

$$s^2 C_1 C_2 \left(1 - \frac{C_1 g_{m01} \tau_1 - g_{m01} g_{m02} \tau_1 \tau_2}{C_1 C_2} \right)$$

$$+ s C_1 g_{m01} \left(1 - \frac{g_{m02} \tau_1}{C_1} \right) + (g_{m01} g_{m02}) \quad (19)$$

The effect of frequency-dependent transconductance can be made negligible by satisfying the following condition:

$$\frac{C_1 g_{m01} \tau_1 - g_{m01} g_{m02} \tau_1 \tau_2}{C_1 C_2} \ll 1 \quad (20)$$

$$\frac{g_{m02} \tau_1}{C_1} \ll 1 \quad (21)$$

III. SIMULATION RESULTS

The MIMO-OTA and the filter were designed and simulated in the Cadence program using 0.18 μ m TSMC CMOS technology. The voltage supply was 0.5V ($V_{DD} = -V_{SS} = 250mV$) and the bias voltage $V_B = -100mV$. The estimated chip area of the MIMO-OTA with one positive and one

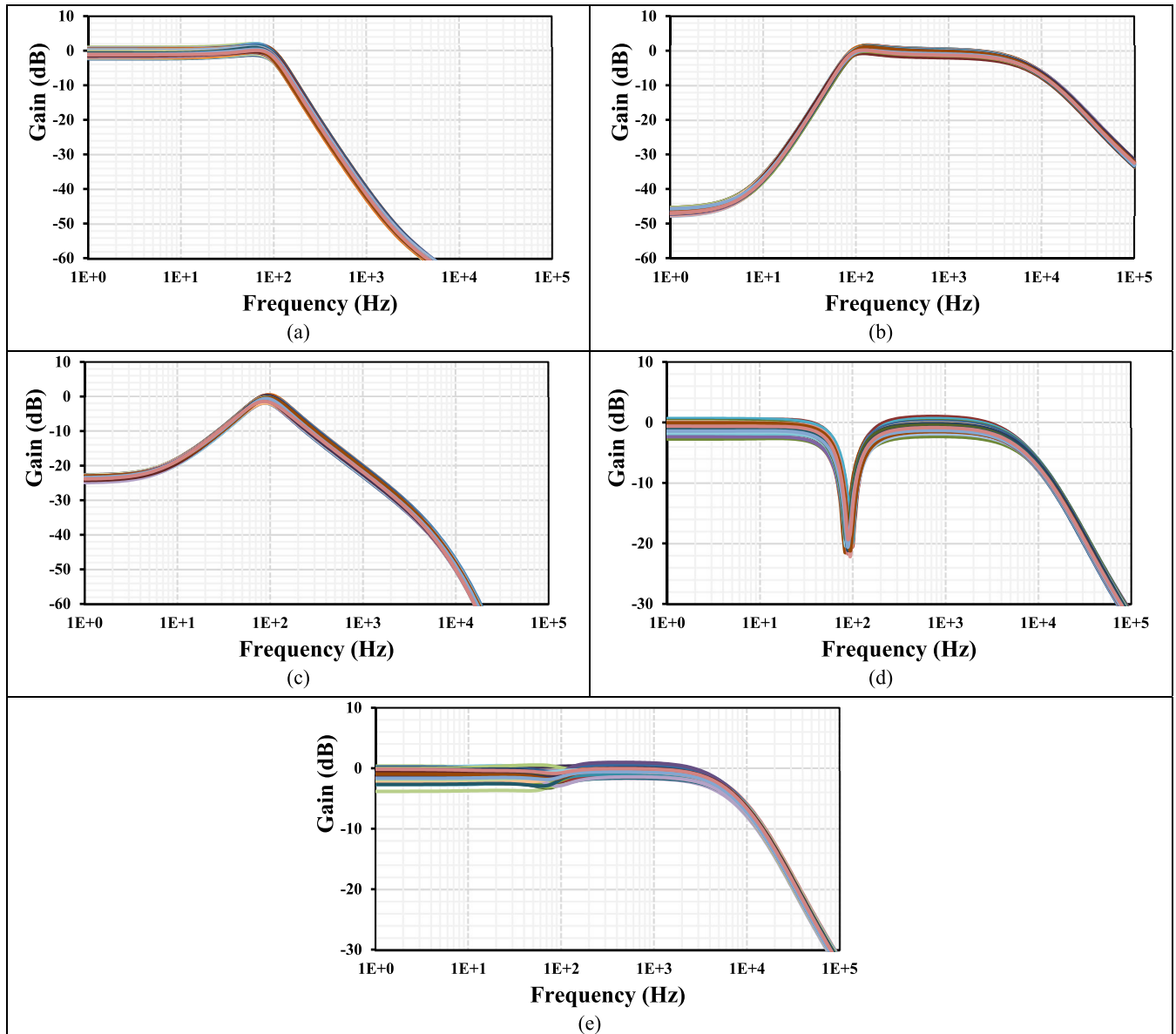


FIGURE 8. The 200 runs MC frequency characteristics of the gains for the VM filter: LPF (a), HPF (b), BPF (c), BSF (d), and APF (e).

negative output (i.e., I_{o+} , I_{o-}) was $116.3 \times 140 \mu\text{m}^2$ and its power consumption was 16nW at a setting current of $I_{\text{set}} = 4\text{nA}$. Each additional output required by the filter increased the power consumption by only 2nW at $I_{\text{set}} = 4\text{nA}$. The transistor aspect ratios are shown in table 2. The input capacitor C_B was realized by a high linear and precision metal-insulator-metal capacitor (MIM) available in TSMC technology.

The DC transfer characteristics of the MIMO-OTA output currents (a) and small-signal transconductances (b) for different $I_{\text{set}} = (2, 4, 8, 16, 32)\text{nA}$ are shown in Fig. 5. The extended linearity is evident and the transconductance values ranged from 6.7 nS to 100nS.

The value of capacitors $C_1 = C_2 = 20\text{pF}$ was chosen for the filter application. The frequency responses for the VM and CM filter were selected to be presented. The frequency responses of the LP, HP, BP, BS, AP gains and phases for VM and CM are shown in Figs. 6 and 7, respectively. The wide tunability of the filter was achieved by varying the setting current $I_{\text{set}1-4} = (2, 4, 8, 16, 32)\text{nA}$. The cutoff frequency was (58.8, 114, 222, 434, 840)Hz, respectively, and the power consumption was in range of 29nW to 464 nW.

Monte Carlo (MC) analysis was used to perform the statistical analysis to estimate the parametric yield and generate information about the performance characteristics of the VM filter. The gains frequency responses of the LP, HP, BP, BS,

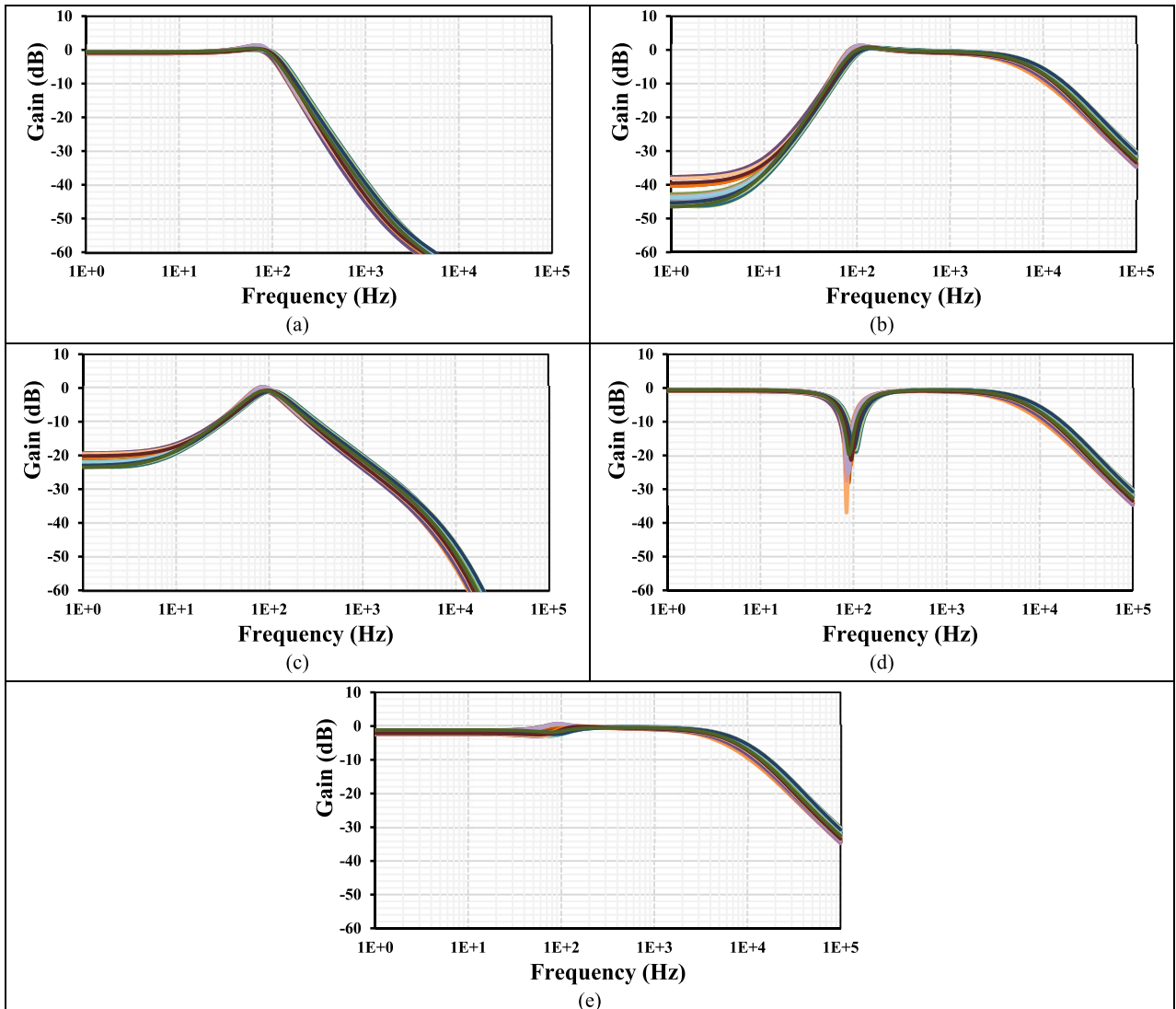


FIGURE 9. The PVT frequency characteristics of the gains for the VM filter: LPF (a), HPF (b), BPF (c), BSF (d), and APF (e).

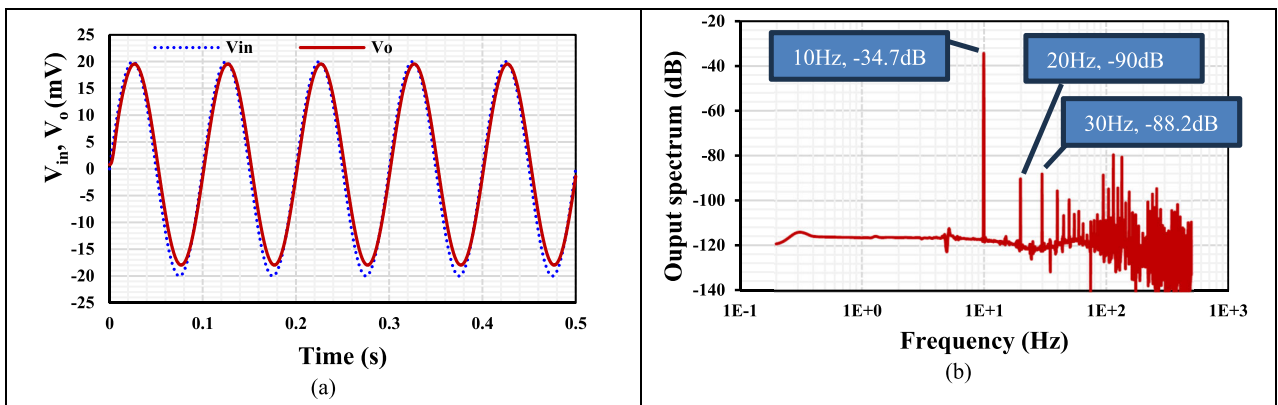


FIGURE 10. The transient response of the VM LPF (a) and the spectrum of the output signal (b).

and AP with 200 runs MC are shown in Fig. 8. The curves are overlapping or close to each other.

The process, voltage, temperature (PVT) corners were also used to confirm the robustness of the design. The process

transistor corners were fast-fast, fast-slow, slow-fast and slow-slow. The process MIM capacitor corners were fast-fast, slow-slow. The voltage supply corners were $\pm 10\%$ (VDD-VSS) and the temperature corners were -20°C and

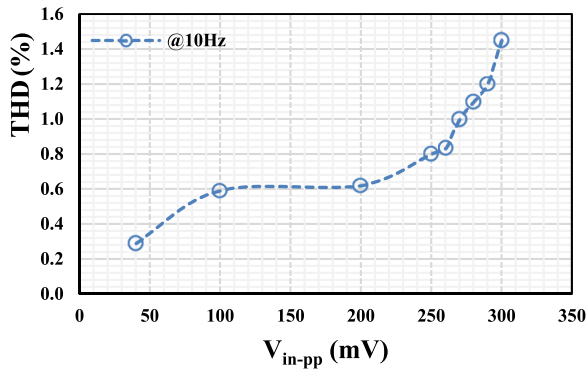


FIGURE 11. The THD of the VM LPF with different peak-to-peak input voltage @ 10Hz.

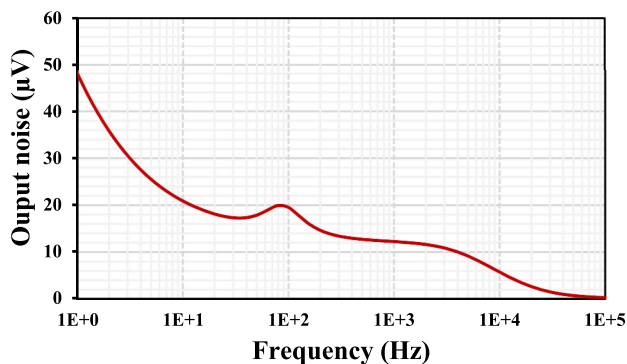


FIGURE 12. The output voltage noise of VM LPF.

70°C. The results for the gains frequency responses of the LP, HP, BP, BS, AP with PVT are shown in Fig. 9. The curves are again overlapping or close to each other that confirm the robustness of the filter design.

The transient response of the VM LPF with the applied input sinusoidal signal $V_{in-pp} = 40\text{mV}@10\text{Hz}$ is shown in Fig. 10 (a). The spectrum of the output signal is shown in Fig. 10 (b), where the total harmonic distortion (THD) of 0.29% is indicated.

The THD for the VM LPF with different peak-to-peak input signal values @ 10Hz is shown in Fig. 11. The 1% THD was achieved for $V_{in-pp} = 270\text{mV}$. The output voltage noise for the VM LPF is shown in Fig. 12. The root-mean square (RMS) output noise integrated in the bandwidth of 1 to 114 Hz was $208\ \mu\text{V}$; thus, the dynamic range (DR) of the VM LPF filter was 53.23dB @ 1% THD.

In table 3, the proposed mixed-mode universal filter is compared to previous works in [5], [17], [18], [23], [35], [37], and [39]. Compared with [5], [17], [18], [23], [35], and [37], the proposed filter offers more transfer functions. Compared with [18], [23], and [37], the proposed filter offers five standard filtering functions of VM, CM, TAM, and TIM. The proposed filter offers electronic tuning ability when compared to [5] and uses fewer active devices when compared to [35] and [39]. Although the filters in [18] and [37] use fewer active devices when compared with the proposed filter,

these filters apply the voltage input signals via the capacitors, thus requiring buffer circuits. Moreover, the filter in [18] requires input matching conditions and inverting input signals, and some output currents of the filter in [37] are supplied via the capacitor and resistor, requiring additional active devices such as a current follower for sensing the currents from these passive devices. Finally, the proposed filter has very low-supply and low-power consumption when compared with [5], [17], [18], [23], [37], and [39].

IV. CONCLUSION

This paper presents an extremely low-voltage low-power mixed-mode universal filter using four MIMO-OTAs and two grounded capacitors. The filter offers VM, CM, TAM, and TIM for LP, HP, BP, BS, and AP responses. This work show that the MIMO-OTA based mixed-mode universal filter offers 35 transfer functions of LP, HP, BP, BS, and AP responses, and thus provides the full capability of a mixed-mode universal filter. Namely, each mode of VM, CM, TAM, and TIM offers five filtering functions. The input voltage terminals and output current terminals of the circuit possess a high-impedance level which is absent from buffer circuit requirements. Moreover, the filter is exempt from inverting input signal requirements; namely, there is no need for additional inverting amplifiers to generate inverting signals. The natural frequency can also be electronically controlled. The voltage supply is 0.5 V and the power consumption of the filter is 58 nW for 4nA setting current. The THD is 1% for $V_{in-pp} = 270\text{mV}$ and the dynamic range is 53.23dB for the VM LPF. The intensive simulation results confirm the functionality of the filter.

REFERENCES

- [1] M. T. Abuelma'atti, A. Bentrchia, and S. M. Al-Shahrani, "A novel mixed-mode current-conveyor-based filter," *Int. J. Electron.*, vol. 91, no. 3, pp. 191–197, Mar. 2004, doi: 10.1080/00207210410001677039.
- [2] M. T. Abuelma'atti and A. Bentrchia, "A novel mixed-mode CCII-based filter," *Act. Passive Electron. Compon.*, vol. 27, no. 4, pp. 197–205, 2004, doi: 10.1080/08827510310001648933.
- [3] C.-N. Lee and C.-M. Chang, "Single FDCCII-based mixed-mode biquad filter with eight outputs," *AEU-Int. J. Electron. Commun.*, vol. 63, no. 9, pp. 736–742, Sep. 2009, doi: 10.1016/j.aeu.2008.06.015.
- [4] S. Minaei and M. A. Ibrahim, "A mixed-mode KHN-biquad using DVCC and grounded passive elements suitable for direct cascading," *Int. J. Circuit Theory Appl.*, vol. 37, no. 7, pp. 793–810, Sep. 2009, doi: 10.1002/cta.493.
- [5] C.-N. Lee, "Fully cascable mixed-mode universal filter biquad using DDCCs and grounded passive components," *J. Circuits, Syst. Comput.*, vol. 20, no. 04, pp. 607–620, Jun. 2011, doi: 10.1142/s0218126611007499.
- [6] W. B. Liao and J. C. Gu, "SIMO type universal mixed-mode biquadratic filter," *Indian J. Eng. Mater. Sci.*, vol. 18, pp. 443–448, 2011.
- [7] C.-N. Lee, "Mixed-mode universal biquadratic filter with no need of matching conditions," *J. Circuits, Syst. Comput.*, vol. 25, no. 9, Sep. 2016, Art. no. 1650106, doi: 10.1142/s0218126616501061.
- [8] C.-N. Lee, "Independently tunable mixed-mode universal biquad filter with versatile input/output functions," *AEU-Int. J. Electron. Commun.*, vol. 70, no. 8, pp. 1006–1019, Aug. 2016, doi: 10.1016/j.aeu.2016.04.006.
- [9] C.-N. Lee, "Mixed-mode universal biquadratic filter with no need of matching conditions," *J. Circuits, Syst. Comput.*, vol. 25, no. 9, Sep. 2016, Art. no. 1650106, doi: 10.1142/s0218126616501061.
- [10] T. Tsukutani, Y. Kinugasa, and N. Yabuki, "A novel mixed-mode universal biquad employing plus current output DVCCs," *Adv. Sci., Technol. Eng. Syst. J.*, vol. 3, no. 4, pp. 236–240, Aug. 2018, doi: 10.25046/aj030423.

- [11] V. K. Singh, A. K. Singh, D. R. Bhaskar, and R. Senani, "Novel mixed-mode universal biquad configuration," *IEICE Electron. Exp.*, vol. 2, no. 22, pp. 548–553, 2005, doi: [10.1587/elex.2.548](https://doi.org/10.1587/elex.2.548).
- [12] N. Pandey, S. K. Paul, A. Bhattacharyya, and S. B. Jain, "A new mixed mode biquad using reduced number of active and passive elements," *IEICE Electron. Exp.*, vol. 3, no. 6, pp. 115–121, 2006, doi: [10.1587/elex.3.115](https://doi.org/10.1587/elex.3.115).
- [13] N. A. Shah and M. F. Rather, "Design of voltage-mode, trans-admittance-mode, trans-impedance-mode and current-mode biquad filter employing plus type current feedback amplifiers," *J. Act. Passive Devices*, vol. 5, no. 1, pp. 29–46, 2010.
- [14] N. A. Shah and M. A. Malik, "Multifunction mixed-mode filter using FTFNs," *Anal. Integr. Circuits Signal Process.*, vol. 47, no. 3, pp. 339–343, Jun. 2006, doi: [10.1007/s10470-006-5539-0](https://doi.org/10.1007/s10470-006-5539-0).
- [15] M. T. Abuelma'atti, "A novel mixed-mode current-controlled current-conveyor-based filter," *Act. Passive Electron. Compon.*, vol. 26, no. 3, pp. 185–191, 2003, doi: [10.1080/1042015031000073841](https://doi.org/10.1080/1042015031000073841).
- [16] L. Zhijun, "Mixed-mode universal filter using MCCCII," *AEU-Int. J. Electron. Commun.*, vol. 63, no. 12, pp. 1072–1075, Dec. 2009, doi: [10.1016/j.aeue.2008.09.003](https://doi.org/10.1016/j.aeue.2008.09.003).
- [17] N. Pandey and S. K. Paul, "Mixed mode universal filter," *J. Circuits, Syst. Comput.*, vol. 22, no. 1, Jan. 2013, Art. no. 1250064, doi: [10.1142/s0218126612500648](https://doi.org/10.1142/s0218126612500648).
- [18] D. Agrawal and S. Maheshwari, "High-performance electronically tunable analog filter using a single EX-CCCII," *Circuits, Syst., Signal Process.*, vol. 40, no. 3, pp. 1127–1151, Mar. 2021, doi: [10.1007/s00034-020-01530-7](https://doi.org/10.1007/s00034-020-01530-7).
- [19] A. Yesil and F. Kacar, "Electronically tunable resistorless mixed-mode biquad filters," *Radioengineering*, vol. 22, no. 4, pp. 1016–1125, 2013.
- [20] S. Maheshwari, S. V. Singh, and D. S. Chauhan, "Electronically tunable low-voltage mixed-mode universal biquad filter," *IET Circuits, Devices Syst.*, vol. 5, pp. 149–158, May 2011, doi: [10.1049/iet-cds.2010.0061](https://doi.org/10.1049/iet-cds.2010.0061).
- [21] M. I. A. Albri, F. Mohammad, N. Herenscar, J. Sampe, and S. H. M. Ali, "Novel electronically tunable biquadratic mixed-mode universal filter capable of operating in MISO and SIMO configurations," *Informacije MIREM*, vol. 50, no. 3, pp. 189–203, 2020, doi: [10.33180/InfMIREM2020.304](https://doi.org/10.33180/InfMIREM2020.304).
- [22] S. V. Singh, R. S. Tomar, and M. Goswami, "A current tunable mixed mode ZC-CCTAs based resistor less universal filter," *J. Circuits, Syst. Comput.*, vol. 30, no. 12, Sep. 2021, Art. no. 2150225, doi: [10.1142/s021812662150225x](https://doi.org/10.1142/s021812662150225x).
- [23] H.-P. Chen and W.-S. Yang, "Electronically tunable current controlled current conveyor transconductance amplifier-based mixed-mode biquadratic filter with resistorless and grounded capacitors," *Appl. Sci.*, vol. 7, no. 3, p. 244, Mar. 2017, doi: [10.3390/app7030244](https://doi.org/10.3390/app7030244).
- [24] M. Faseehuddin, N. Herenscar, M. A. Albri, S. Shireen, and J. Sampe, "Electronically tunable mixed mode universal filter employing grounded capacitors utilizing highly versatile VD-DVCC," *Circuit World*, vol. 48, no. 4, pp. 511–528, Nov. 2022, doi: [10.1108/cw-05-2020-0080](https://doi.org/10.1108/cw-05-2020-0080).
- [25] R. Mishra, G. R. Mishra, S. O. Mishra, and M. Faseehuddin, "Electronically tunable mixed mode universal filter employing grounded passive components," *Informacije MIREM*, vol. 52, no. 2, pp. 105–115, 2022, doi: [10.33180/InfMIREM2022.204](https://doi.org/10.33180/InfMIREM2022.204).
- [26] M. T. Abuelma'atti and A. Bentrchia, "A novel mixed-mode OTA-C universal filter," *Int. J. Electron.*, vol. 92, no. 7, pp. 375–383, Jul. 2005, doi: [10.1080/08827510412331295009](https://doi.org/10.1080/08827510412331295009).
- [27] D. R. Bhaskar, A. K. Singh, R. K. Sharma, and R. Senani, "New OTA-C universal current-mode/trans-admittance biquads," *IEICE Electron. Exp.*, vol. 2, no. 1, pp. 8–13, 2005.
- [28] H.-P. Chen, Y.-Z. Liao, and W.-T. Lee, "Tunable mixed-mode OTA-C universal filter," *Anal. Integr. Circuits Signal Process.*, vol. 58, no. 2, pp. 135–141, Feb. 2009, doi: [10.1007/s10470-008-9228-z](https://doi.org/10.1007/s10470-008-9228-z).
- [29] C.-N. Lee, "Multiple-mode OTA-C universal biquad filters," *Circuits, Syst. Signal Process.*, vol. 29, no. 2, pp. 263–274, Apr. 2010, doi: [10.1007/s00034-009-9145-0](https://doi.org/10.1007/s00034-009-9145-0).
- [30] M. Kummern and S. Jannapiya, "Mixed-mode universal filter using OTAs," in *Proc. IEEE Int. Conf. Cyber Technol. Autom., Control, Intell. Syst. (CYBER)*, Bangkok, Thailand, May 2012, pp. 119–122, doi: [10.1109/CYBER.2012.6392537](https://doi.org/10.1109/CYBER.2012.6392537).
- [31] S. M. A. Zanjani, M. Dousti, and M. Dolatshahi, "Inverter-based, low-power and low-voltage, new mixed-mode Gm-C filter in subthreshold CNTFET technology," *IET Circuits, Devices Syst.*, vol. 12, no. 6, pp. 681–688, Nov. 2018, doi: [10.1049/iet-cds.2018.5158](https://doi.org/10.1049/iet-cds.2018.5158).
- [32] M. Parvizi, A. Taghizadeh, H. Mahmoodian, and Z. D. Kozehkanani, "A low-power mixed-mode SIMO universal Gm-C filter," *J. Circuits, Syst. Comput.*, vol. 26, no. 10, Oct. 2017, Art. no. 1750164, doi: [10.1142/s021812661750164x](https://doi.org/10.1142/s021812661750164x).
- [33] M. Parvizi, "Design of a new low power MISO multi-mode universal biquad OTA-C filter," *Int. J. Electron.*, vol. 106, no. 3, pp. 440–454, Mar. 2019, doi: [10.1080/00207217.2018.1540064](https://doi.org/10.1080/00207217.2018.1540064).
- [34] D. R. Bhaskar, A. Raj, and P. Kumar, "Mixed-mode universal biquad filter using OTAs," *J. Circuits, Syst. Comput.*, vol. 29, no. 10, Aug. 2020, Art. no. 2050162, doi: [10.1142/s0218126620501625](https://doi.org/10.1142/s0218126620501625).
- [35] A. Namdari and M. Dolatshahi, "Design of a low-voltage and low-power, reconfigurable universal OTA-C filter," *Analog Integr. Circuits Signal Process.*, vol. 111, pp. 169–188, Feb. 2022, doi: [10.1007/s10470-022-01996-2](https://doi.org/10.1007/s10470-022-01996-2).
- [36] M. Faseehuddin, N. Herenscar, S. Shireen, W. Tangsrirat, and S. H. M. Ali, "Voltage differencing buffered amplifier-based novel truly mixed-mode biquadratic universal filter with versatile input/output features," *Appl. Sci.*, vol. 12, no. 3, p. 1229, Jan. 2022, doi: [10.3390/app12031229](https://doi.org/10.3390/app12031229).
- [37] N. Roongmuanpha, M. Faseehuddin, N. Herenscar, and W. Tangsrirat, "Tunable mixed-mode voltage differencing buffered amplifier-based universal filter with independently high-Q factor controllability," *Appl. Sci.*, vol. 11, no. 20, p. 9606, Oct. 2021, doi: [10.3390/app11209606](https://doi.org/10.3390/app11209606).
- [38] N. Roongmuanpha, W. Tangsrirat, and T. Pukkalanun, "Single VDGA-based mixed-mode universal filter and dual-mode quadrature oscillator," *Sensors*, vol. 22, no. 14, p. 5303, Jul. 2022, doi: [10.3390/s22145303](https://doi.org/10.3390/s22145303).
- [39] M. Kummern, P. Suksaibul, F. Khateb, and T. Kulej, "1.2 V differential difference transconductance amplifier and its application in mixed-mode universal filter," *Sensors*, vol. 22, no. 9, p. 3535, May 2022, doi: [10.3390/s22093535](https://doi.org/10.3390/s22093535).
- [40] E. Sackinger and W. Guggenbuhl, "A versatile building block: The CMOS differential difference amplifier," *IEEE J. Solid-State Circuits*, vol. 22, no. 2, pp. 287–294, Apr. 1987, doi: [10.1109/jssc.1987.1052715](https://doi.org/10.1109/jssc.1987.1052715).
- [41] S.-C. Huang, M. Ismail, and S. R. Zarabadi, "A wide range differential difference amplifier: A basic block for analog signal processing in MOS technology," *IEEE Trans. Circuits Syst. II, Analog Digit. Signal Process.*, vol. 40, no. 5, pp. 289–301, May 1993, doi: [10.1109/82.227369](https://doi.org/10.1109/82.227369).
- [42] S. R. Zarabadi, F. Larsen, and M. Ismail, "A reconfigurable op-amp/DDA CMOS amplifier architecture," *IEEE Trans. Circuits Syst. I, Fundam. Theory Appl.*, vol. 39, no. 6, pp. 484–487, Jun. 1992, doi: [10.1109/81.153646](https://doi.org/10.1109/81.153646).
- [43] Z. Czarnul, S. Takagi, and N. Fujii, "Common-mode feedback circuit with differential-difference amplifier," *IEEE Trans. Circuits Syst. I, Fundam. Theory Appl.*, vol. 41, no. 3, pp. 243–246, Mar. 1994, doi: [10.1109/81.273924](https://doi.org/10.1109/81.273924).
- [44] J. F. Duque-Carrillo, G. Torelli, R. Perez-Aloe, J. M. Valverde, and F. Maloberti, "Fully differential basic building blocks based on fully differential difference amplifiers with unity-gain difference feedback," *IEEE Trans. Circuits Syst. I, Fundam. Theory Appl.*, vol. 42, no. 3, pp. 190–192, Mar. 1995, doi: [10.1109/81.376865](https://doi.org/10.1109/81.376865).
- [45] W. Chiu, S.-I. Liu, H.-W. Tsao, and J.-J. Chen, "CMOS differential difference current conveyors and their applications," *IEE Proc.-Circuits, Devices Syst.*, vol. 143, no. 2, pp. 91–96, 1996, doi: [10.1049/ip-cds:19960223](https://doi.org/10.1049/ip-cds:19960223).
- [46] H. O. Elwan and A. M. Soliman, "Novel CMOS differential voltage current conveyor and its applications," *IEE Proc.-Circuits, Devices Syst.*, vol. 144, no. 3, pp. 195–200, 1997, doi: [10.1049/ip-cds:19971081](https://doi.org/10.1049/ip-cds:19971081).
- [47] S. A. Mahmoud and A. M. Soliman, "The differential difference operational floating amplifier: A new block for analog signal processing in MOS technology," *IEEE Trans. Circuits Syst. II, Analog Digit. Signal Process.*, vol. 45, no. 1, pp. 148–158, 1998, doi: [10.1109/82.659468](https://doi.org/10.1109/82.659468).
- [48] A. Wyszynski and R. Schaumann, "Using multiple-input transconductors to reduce number of components in OTA-C filter design," *Electron. Lett.*, vol. 28, no. 3, pp. 217–220, 1992, doi: [10.1049/el:19920135](https://doi.org/10.1049/el:19920135).
- [49] D. H. Chiang and R. Schaumann, "A CMOS fully-balanced continuous-time IFLF filter design for read/write channels," in *Proc. IEEE Int. Symp. Circuits Syst. Connecting World (ISCAS)*, Atlanta, GA, USA, vol. 1, May 1996, pp. 167–170, doi: [10.1109/ISCAS.1996.539835](https://doi.org/10.1109/ISCAS.1996.539835).
- [50] V. Gopinathan, Y. P. Tsvividis, K.-S. Tan, and R. K. Hester, "Design considerations for high-frequency continuous-time filters and implementation of an antialiasing filter for digital video," *IEEE J. Solid-State Circuits*, vol. 25, no. 6, pp. 1368–1378, Dec. 1990, doi: [10.1109/4.62164](https://doi.org/10.1109/4.62164).
- [51] J. Glinianowicz, J. Jakusz, S. Szczepanski, and Y. Sun, "High-frequency two-input CMOS OTA for continuous-time filter applications," *IEE Proc.-Circuits, Devices Syst.*, vol. 147, no. 1, pp. 13–18, 2000, doi: [10.1049/ip-cds:20000317](https://doi.org/10.1049/ip-cds:20000317).

- [52] F. Khateb, T. Kulej, M. Kumngern, and C. Psychalinos, "Multiple-input bulk-driven MOS transistor for low-voltage low-frequency applications," *Circuits, Syst., Signal Process.*, vol. 38, no. 6, pp. 2829–2845, Jun. 2019, doi: [10.1007/s00034-018-9999-x](https://doi.org/10.1007/s00034-018-9999-x).
- [53] F. Khateb, T. Kulej, H. Veldandi, and W. Jaikla, "Multiple-input bulk-driven quasi-floating-gate MOS transistor for low-voltage low-power integrated circuits," *AEU-Int. J. Electron. Commun.*, vol. 100, pp. 32–38, Feb. 2019, doi: [10.1016/j.aeue.2018.12.023](https://doi.org/10.1016/j.aeue.2018.12.023).
- [54] F. Khateb, T. Kulej, M. Kumngern, W. Jaikla, and R. K. Ranjan, "Comparative performance study of multiple-input bulk-driven and multiple-input bulk-driven quasi-floating-gate DDCCs," *AEU-Int. J. Electron. Commun.*, vol. 108, pp. 19–28, Aug. 2019, doi: [10.1016/j.aeue.2019.06.003](https://doi.org/10.1016/j.aeue.2019.06.003).
- [55] F. Khateb, T. Kulej, M. Akbari, and K.-T. Tang, "A 0.5-V multiple-input bulk-driven OTA in 0.18- μm CMOS," *IEEE Trans. Very Large Scale Integr. (VLSI) Syst.*, vol. 30, no. 11, pp. 1739–1747, Nov. 2022, doi: [10.1109/TVLSI.2022.3203148](https://doi.org/10.1109/TVLSI.2022.3203148).
- [56] F. Khateb, M. Kumngern, T. Kulej, M. Akbari, and V. Stopjakova, "0.5 V, nW-range universal filter based on multiple-input transconductor for biosignals processing," *Sensors*, vol. 22, no. 22, p. 8619, Nov. 2022, doi: [10.3390/s22228619](https://doi.org/10.3390/s22228619).
- [57] F. Khateb, M. Kumngern, T. Kulej, and M. Yavari, "0.5-V nano-power shadow sinusoidal oscillator using bulk-driven multiple-input operational transconductance amplifier," *Sensors*, vol. 23, no. 4, p. 2146, Feb. 2023, doi: [10.3390/s23042146](https://doi.org/10.3390/s23042146).
- [58] F. Khateb, M. Kumngern, and T. Kulej, "0.5-V nano-power voltage-mode first-order universal filter based on multiple-input OTA," *IEEE Access*, vol. 11, pp. 49806–49818, 2023, doi: [10.1109/ACCESS.2023.3277252](https://doi.org/10.1109/ACCESS.2023.3277252).
- [59] M. Kumngern, F. Khateb, and T. Kulej, "Extremely low-voltage low-power differential difference current conveyor using multiple-input bulk-driven technique," *AEU-Int. J. Electron. Commun.*, vol. 123, Aug. 2020, Art. no. 153310, doi: [10.1016/j.aeue.2020.153310](https://doi.org/10.1016/j.aeue.2020.153310).
- [60] M. Kumngern, F. Khateb, and T. Kulej, "0.3 V differential difference current conveyor using multiple-input bulk-driven technique," *Circuits, Syst., Signal Process.*, vol. 39, no. 6, pp. 3189–3205, Jun. 2020, doi: [10.1007/s00034-019-01292-x](https://doi.org/10.1007/s00034-019-01292-x).
- [61] F. Khateb, M. Kumngern, T. Kulej, and C. Psychalinos, "0.5 V universal filter based on multiple-input FDDAs," *Circuits, Syst., Signal Process.*, vol. 38, no. 12, pp. 5896–5907, Dec. 2019, doi: [10.1007/s00034-019-01147-5](https://doi.org/10.1007/s00034-019-01147-5).
- [62] M. Kumngern, N. Aupithak, F. Khateb, and T. Kulej, "0.5 V fifth-order Butterworth low-pass filter using multiple-input OTA for ECG applications," *Sensors*, vol. 20, no. 24, p. 7343, Dec. 2020, doi: [10.3390/s20247343](https://doi.org/10.3390/s20247343).
- [63] M. Kumngern, T. Kulej, F. Khateb, V. Stopjakova, and R. K. Ranjan, "Nanopower multiple-input DTMOS OTA and its applications to high-order filters for biomedical systems," *AEU-Int. J. Electron. Commun.*, vol. 130, Feb. 2021, Art. no. 153576, doi: [10.1016/j.aeue.2020.153576](https://doi.org/10.1016/j.aeue.2020.153576).
- [64] M. Kumngern, T. Kulej, V. Stopjakova, and F. Khateb, "0.5 V sixth-order Chebyshev band-pass filter based on multiple-input bulk-driven OTA," *AEU-Int. J. Electron. Commun.*, vol. 111, Nov. 2019, Art. no. 152930, doi: [10.1016/j.aeue.2019.152930](https://doi.org/10.1016/j.aeue.2019.152930).
- [65] W. Jaikla, F. Khateb, M. Kumngern, T. Kulej, R. K. Ranjan, and P. Suwanjan, "0.5 V fully differential universal filter based on multiple input OTAs," *IEEE Access*, vol. 8, pp. 187832–187839, 2020, doi: [10.1109/ACCESS.2020.3030239](https://doi.org/10.1109/ACCESS.2020.3030239).
- [66] M. Kumngern, F. Khateb, T. Kulej, and C. Psychalinos, "Multiple-input universal filter and quadrature oscillator using multiple-input operational transconductance amplifiers," *IEEE Access*, vol. 9, pp. 56253–56263, 2021, doi: [10.1109/ACCESS.2021.3071829](https://doi.org/10.1109/ACCESS.2021.3071829).
- [67] F. Krummenacher and N. Joehl, "A 4-MHz CMOS continuous-time filter with on-chip automatic tuning," *IEEE J. Solid-State Circuits*, vol. 23, no. 3, pp. 750–758, Jun. 1988, doi: [10.1109/4.315](https://doi.org/10.1109/4.315).
- [68] H. Nevárez-Lozano and E. Sánchez-Sinencio, "Minimum parasitic effects biquadratic OTA-C filter architectures," *Anal. Integr. Circuits Signal Process.*, vol. 1, no. 4, pp. 297–319, Dec. 1991, doi: [10.1007/bf00239678](https://doi.org/10.1007/bf00239678).



FABIAN KHATEB received the dual M.Sc. and dual Ph.D. degrees in electrical engineering and communication and in business and management from the Brno University of Technology, Czech Republic, in 2002, 2003, 2005, and 2007, respectively. He is currently a Professor with the Department of Microelectronics, Faculty of Electrical Engineering and Communication, Brno University of Technology; the Department of Electrical Engineering, University of Defence, Brno; and the

Department of Information and Communication Technology in Medicine, Faculty of Biomedical Engineering, Czech Technical University in Prague. He holds five patents. He has authored or coauthored over 140 publications in journals and proceedings of international conferences. His expertise is in new principles of designing low-voltage low-power analog circuits, particularly for biomedical applications. He is an Editorial Board Member of the *Microelectronics Journal*, *Sensors*, *Machines*, *Electronics*, and *Journal of Low Power Electronics and Applications*. He is an Associate Editor of IEEE Access, *Circuits, Systems, and Signal Processing*, *IET Circuits, Devices and Systems*, and *International Journal of Electronics*. He was a Lead Guest Editor of the *Circuits, Systems, and Signal Processing* Special Issue on Low Voltage Integrated Circuits and Systems, in 2017; *IET Circuits, Devices and Systems*, in 2018; and *Microelectronics Journal*, in 2019. He was also a Guest Editor of the Special Issue on Current-Mode Circuits and Systems; and Recent Advances, Design and Applications on *International Journal of Electronics and Communications*, in 2017.



MONTREE KUMNGERN received the B.S.Ind.Ed. degree from the King Mongkut's University of Technology Thonburi, Thailand, in 1998, and the M.Eng. and D.Eng. degrees from the King Mongkut's Institute of Technology Ladkrabang, Thailand, in 2002 and 2006, respectively, all in electrical engineering. In 2007, he was a Lecturer with the Department of Telecommunications Engineering, Faculty of Engineering, King Mongkut's Institute of Technology Ladkrabang,

where he was an Assistant Professor, from 2010 to 2017, and currently an Associate Professor. He has authored or coauthored over 200 publications in journals and proceedings of international conferences. His research interests include analog and digital integrated circuits, discrete-time analog filters, non-linear circuits, data converters, and ultra-low voltage building blocks for biomedical applications.

TOMASZ KULEJ received the M.Sc. and Ph.D. degrees from the Gdańsk University of Technology, Gdańsk, Poland, in 1990 and 1996, respectively. He was a Senior Design Analysis Engineer with Polish Branch of Chipworks Inc., Ottawa, Canada. He is currently an Associate Professor with the Department of Electrical Engineering, Częstochowa University of Technology, Poland, where he conducts lectures on electronics fundamentals, analog circuits, and computer



aided design. He has authored or coauthored over 100 publications in peer-reviewed journals and conferences. He holds three patents. His current research interests include analog integrated circuits in CMOS technology, with an emphasis on low voltage and low power solutions. He serves as an Associate Editor for the *Circuits, Systems, and Signal Processing* and *IET Circuits, Devices and Systems*. He was a Guest Editor of the *Circuits, Systems, and Signal Processing* Special Issue on Low Voltage Integrated Circuits, in 2017; *IET Circuits, Devices and Systems*, in 2018; and *Microelectronics Journal*, in 2019.

...